
VARIATIONAL PERTURBATION THEORY FOR THE GROUND-STATE WAVE FUNCTION

A. PELSTER AND F. WEISSBACH

*Institut für Theoretische Physik, Freie Universität Berlin,
Arnimallee 14, D-14195 Berlin, Germany*

E-mails: pelster@physik.fu-berlin.de, florian.weissbach@physik.fu-berlin.de

We evaluate perturbatively the density matrix in the low-temperature limit and thus the ground-state wave function of the anharmonic oscillator up to second order in the coupling constant. We then employ Kleinert's variational perturbation theory to determine the ground-state wave function for all coupling strengths.

1 Introduction

Variational perturbation theory as developed by Kleinert [1] provides a systematic algorithm to evaluate perturbation series at all coupling strengths including the strong-coupling limit $g \rightarrow \infty$. It was thoroughly investigated for the ground-state energy of the anharmonic oscillator up to the 250th order [2,3], and its convergence was found to be exponentially fast and uniform. A similar systematic study has not yet been performed for the ground-state wave function. A first-order variational approach was set up by Kunihiro [4]. However, his method did not satisfactorily deal with certain problems in the variational procedure which will be discussed in detail below.

In this work we improve Kunihiro's first-order calculation and extend the treatment to the second order in the coupling strength. The ground-state wave function of the anharmonic oscillator is calculated from the low-temperature limit of the diagonal elements of the density matrix. A variational evaluation of the density matrix for the double-well potential has already been performed for finite temperatures in Ref. [5].

2 Perturbation Theory

Consider a quantum mechanical point particle of mass M moving in the one-dimensional anharmonic oscillator potential

$$V(x) = \frac{M}{2}\omega^2 x^2 + gx^4, \quad (1)$$

where ω denotes the frequency and g the coupling constant. We determine its ground-state wave function $\Psi(x)$ by evaluating the low-temperature limit of the diagonal elements of the density matrix

$$\Psi(x) = \lim_{\beta \rightarrow \infty} \sqrt{\rho(x, x)}, \quad (2)$$

which is defined by

$$\rho(x_b, x_a) = \frac{(x_b \hbar\beta | x_a 0)}{Z}. \quad (3)$$

Here $(x_b \hbar\beta | x_a 0)$ denotes the imaginary-time evolution amplitude with the path-integral representation [1]

$$\begin{aligned} (x_b \hbar\beta | x_a 0) &= \int_{x(0)=x_a}^{x(\hbar\beta)=x_b} \mathcal{D}x \\ &\times \exp \left\{ -\frac{1}{\hbar} \int_0^{\hbar\beta} d\tau \left[\frac{M}{2} \dot{x}^2(\tau) + \frac{M}{2} \omega^2 x^2(\tau) + gx^4(\tau) \right] \right\}, \quad (4) \end{aligned}$$

and Z denotes the partition function

$$Z = \int_{-\infty}^{+\infty} dx (x \hbar\beta | x 0). \quad (5)$$

By expanding Eq. (4) in powers of the coupling constant g we obtain the perturbation series

$$\begin{aligned} (x_b \hbar\beta | x_a 0) &= (x_b \hbar\beta | x_a 0)_\omega \left[1 - \frac{g}{\hbar} \int_0^{\hbar\beta} d\tau_1 \langle x^4(\tau_1) \rangle_\omega \right. \\ &\left. + \frac{g^2}{2\hbar^2} \int_0^{\hbar\beta} d\tau_1 \int_0^{\hbar\beta} d\tau_2 \langle x^4(\tau_1) x^4(\tau_2) \rangle_\omega + \dots \right], \quad (6) \end{aligned}$$

where we have introduced the harmonic imaginary-time evolution amplitude

$$(x_b \hbar\beta | x_a 0)_\omega \equiv \int_{x(0)=x_a}^{x(\hbar\beta)=x_b} \mathcal{D}x \times \exp \left\{ -\frac{1}{\hbar} \int_0^{\hbar\beta} d\tau \left[\frac{M}{2} \dot{x}^2(\tau) + \frac{M}{2} \omega^2 x^2(\tau) \right] \right\}, \quad (7)$$

and the harmonic expectation value for an arbitrary functional $F[x]$ of the path $x(\tau)$:

$$\langle F[x] \rangle_\omega \equiv \frac{1}{(x_b \hbar\beta | x_a 0)_\omega} \int_{x(0)=x_a}^{x(\hbar\beta)=x_b} \mathcal{D}x F[x] \times \exp \left\{ -\frac{1}{\hbar} \int_0^{\hbar\beta} d\tau \left[\frac{M}{2} \dot{x}^2(\tau) + \frac{M}{2} \omega^2 x^2(\tau) \right] \right\}. \quad (8)$$

The latter is evaluated with the help of the generating functional for the harmonic oscillator, whose path-integral representation reads

$$(x_b \hbar\beta | x_a 0)_\omega [j] = \int_{x(0)=x_a}^{x(\hbar\beta)=x_b} \mathcal{D}x \exp \left\{ -\frac{1}{\hbar} \int_0^{\hbar\beta} d\tau \left[\frac{M}{2} \dot{x}^2(\tau) + \frac{M}{2} \omega^2 x^2(\tau) - j(\tau)x(\tau) \right] \right\}, \quad (9)$$

leading to [1]

$$(x_b \hbar\beta | x_a 0)_\omega [j] = (x_b \hbar\beta | x_a 0)_\omega \exp \left[\frac{1}{\hbar} \int_0^{\hbar\beta} d\tau_1 x_{cl}(\tau_1) j(\tau_1) + \frac{1}{2\hbar^2} \int_0^{\hbar\beta} d\tau_1 \int_0^{\hbar\beta} d\tau_2 G(\tau_1, \tau_2) j(\tau_1) j(\tau_2) \right], \quad (10)$$

with

$$(x_b \hbar\beta | x_a 0)_\omega = \sqrt{\frac{M\omega}{2\pi\hbar \sinh \hbar\beta\omega}} \times \exp \left\{ -\frac{M\omega}{2\hbar \sinh \hbar\beta\omega} [(x_a^2 + x_b^2) \cosh \hbar\beta\omega - 2x_a x_b] \right\}. \quad (11)$$

In Eq. (10) we have introduced the classical path

$$x_{\text{cl}}(\tau) \equiv \frac{x_a \sinh(\hbar\beta - \tau)\omega + x_b \sinh \omega\tau}{\sinh \hbar\beta\omega}, \quad (12)$$

and the Green function

$$G(\tau_1, \tau_2) \equiv \frac{\hbar}{2M\omega \sinh \hbar\beta\omega} [\theta(\tau_1 - \tau_2) \sinh(\hbar\beta - \tau_1)\omega \sinh \omega\tau_2 + \theta(\tau_2 - \tau_1) \sinh(\hbar\beta - \tau_2)\omega \sinh \omega\tau_1]. \quad (13)$$

We follow Ref. [6] and evaluate harmonic expectation values of polynomials in x arising from the generating functional (10) according to Wick's theorem. Let us illustrate the procedure to reduce the power of the polynomial by the example of the harmonic expectation value

$$\langle x^n(\tau_1) x^m(\tau_2) \rangle_\omega. \quad (14)$$

- (i) Contracting $x(\tau_1)$ with $x^{n-1}(\tau_1)$ and $x^m(\tau_2)$ leads to a Green function $G(\tau_1, \tau_1)$ and $G(\tau_1, \tau_2)$ with multiplicity $n-1$ and m , respectively. The rest of the polynomial remains within the harmonic expectation value, leading to $\langle x^{n-2}(\tau_1) x^m(\tau_2) \rangle_\omega$ and $\langle x^{n-1}(\tau_1) x^{m-1}(\tau_2) \rangle_\omega$.
- (ii) If $n > 1$, extract one $x(\tau_1)$ from the expectation value giving $x_{\text{cl}}(\tau_1)$ multiplied by $\langle x^{n-1}(\tau_1) x^m(\tau_2) \rangle_\omega$.
- (iii) Add the terms (i) and (ii).
- (iv) Repeat the previous steps until only products of expectation values $\langle x(\tau_1) \rangle_\omega = x_{\text{cl}}(\tau_1)$ remain.

With the help of this procedure, the first-order harmonic expectation value $\langle x^4(\tau_1) \rangle_\omega$ is reduced to

$$\langle x^4(\tau_1) \rangle_\omega = x_{\text{cl}}(\tau_1) \langle x^3(\tau_1) \rangle_\omega + 3 G(\tau_1, \tau_1) \langle x^2(\tau_1) \rangle_\omega. \quad (15)$$

Furthermore, we find

$$\langle x^3(\tau_1) \rangle_\omega = x_{\text{cl}}(\tau_1) \langle x^2(\tau_1) \rangle_\omega + 2G(\tau_1, \tau_1) x_{\text{cl}}(\tau_1) \quad (16)$$

and

$$\langle x^2(\tau_1) \rangle_\omega = x_{\text{cl}}^2(\tau_1) + G(\tau_1, \tau_1). \quad (17)$$

Combining Eqs. (15)–(17) we obtain in first order

$$\langle x^4(\tau_1) \rangle_\omega = x_{\text{cl}}^4(\tau_1) + 6 x_{\text{cl}}^2(\tau_1) G(\tau_1, \tau_1) + 3 G^2(\tau_1, \tau_1). \quad (18)$$

The second-order harmonic expectation value requires considerably more effort and finally leads to

$$\begin{aligned}
 \langle x^4(\tau_1) x^4(\tau_2) \rangle_\omega &= x_{\text{cl}}^4(\tau_1) x_{\text{cl}}^4(\tau_2) + 16 x_{\text{cl}}^3(\tau_1) G(\tau_1, \tau_2) x_{\text{cl}}^3(\tau_2) \\
 &+ 12 x_{\text{cl}}^2(\tau_1) G(\tau_1, \tau_1) x_{\text{cl}}^4(\tau_2) + 72 x_{\text{cl}}^2(\tau_1) G^2(\tau_1, \tau_2) x_{\text{cl}}^2(\tau_2) \\
 &+ 36 x_{\text{cl}}^2(\tau_1) G(\tau_1, \tau_1) G(\tau_2, \tau_2) x_{\text{cl}}^2(\tau_2) + 96 x_{\text{cl}}^3(\tau_1) G(\tau_1, \tau_2) G(\tau_2, \tau_2) x_{\text{cl}}(\tau_2) \\
 &+ 6 G^2(\tau_1, \tau_1) x_{\text{cl}}^4(\tau_2) + 96 x_{\text{cl}}(\tau_1) G^3(\tau_1, \tau_2) x_{\text{cl}}(\tau_2) \\
 &+ 144 x_{\text{cl}}(\tau_1) G(\tau_1, \tau_1) G(\tau_1, \tau_2) G(\tau_2, \tau_2) x_{\text{cl}}(\tau_2) + 9 G^2(\tau_1, \tau_1) G^2(\tau_2, \tau_2) \\
 &+ 36 G^2(\tau_1, \tau_1) x_{\text{cl}}^2(\tau_2) G(\tau_2, \tau_2) + 144 x_{\text{cl}}^2(\tau_1) G^2(\tau_1, \tau_2) G(\tau_2, \tau_2) \\
 &+ 72 G(\tau_1, \tau_1) G^2(\tau_1, \tau_2) G(\tau_2, \tau_2) + 24 G^4(\tau_1, \tau_2). \quad (19)
 \end{aligned}$$

The contractions can be illustrated by Feynman diagrams with the following rules. A vertex represents the integration over τ

$$\times = \int_0^{\hbar\beta} d\tau, \quad (20)$$

a line denotes the Green function

$$1 \text{ --- } 2 = G(\tau_1, \tau_2), \quad (21)$$

and a cross pictures a classical path

$$\times \text{ --- } 1 = x_{\text{cl}}(\tau_1). \quad (22)$$

Inserting the harmonic expectation values (18) and (19) into the perturbation expansion (6) leads in first order to the diagrams

$$\int_0^{\hbar\beta} d\tau_1 \langle x^4(\tau_1) \rangle_\omega \equiv \times \begin{array}{c} \times \\ | \\ \times \\ | \\ \times \end{array} \times + 6 \times \begin{array}{c} \times \\ | \\ \times \\ | \\ \times \end{array} \begin{array}{c} \circ \\ \times \end{array} \times + 3 \begin{array}{c} \circ \\ \times \end{array} \begin{array}{c} \circ \\ \times \end{array}, \quad (23)$$

whereas the second-order terms are

$$\begin{aligned}
 \int_0^{\hbar\beta} d\tau_1 \int_0^{\hbar\beta} d\tau_2 \langle x^4(\tau_1) x^4(\tau_2) \rangle_\omega &\equiv \times \begin{array}{c} \times \\ | \\ \times \\ | \\ \times \end{array} \times \times \begin{array}{c} \times \\ | \\ \times \\ | \\ \times \end{array} \times + 16 \times \begin{array}{c} \times \\ | \\ \times \\ | \\ \times \end{array} \begin{array}{c} \times \\ | \\ \times \\ | \\ \times \end{array} \times \\
 &+ 12 \times \begin{array}{c} \circ \\ \times \end{array} \times \times \begin{array}{c} \times \\ | \\ \times \\ | \\ \times \end{array} \times + 72 \times \begin{array}{c} \times \\ | \\ \times \\ | \\ \times \end{array} \begin{array}{c} \times \\ | \\ \times \\ | \\ \times \end{array} \times \\
 &+ 36 \times \begin{array}{c} \circ \\ \times \end{array} \times \times \begin{array}{c} \circ \\ \times \end{array} \times
 \end{aligned}$$

$$\begin{aligned}
 & +96 \times \begin{array}{c} \times \\ | \\ \times \end{array} \begin{array}{c} \circ \\ | \\ \times \end{array} + 6 \begin{array}{c} \circ \\ \circ \end{array} \times \begin{array}{c} \times \\ | \\ \times \end{array} + 96 \times \begin{array}{c} \circ \\ | \\ \times \end{array} \\
 & +144 \times \begin{array}{c} \circ \\ | \\ \times \end{array} \begin{array}{c} \circ \\ | \\ \times \end{array} + 36 \begin{array}{c} \circ \\ \circ \end{array} \times \begin{array}{c} \circ \\ | \\ \times \end{array} + 144 \begin{array}{c} \times \\ \diagdown \\ \times \end{array} \begin{array}{c} \circ \\ \circ \end{array} \\
 & +72 \begin{array}{c} \circ \\ \circ \\ \circ \end{array} + 24 \begin{array}{c} \circ \\ \circ \end{array} + 9 \begin{array}{c} \circ \\ \circ \end{array} \begin{array}{c} \circ \\ \circ \end{array} . \quad (24)
 \end{aligned}$$

We observe that contributions from both connected and disconnected Feynman diagrams appear. The disconnected diagrams vanish once we rewrite the imaginary-time evolution amplitude in the form

$$(x_b \hbar\beta | x_a 0) = (x_b \hbar\beta | x_a 0)_\omega \exp [W(x_b, \hbar\beta; x_a, 0)] , \quad (25)$$

where the exponent $W(x_b, \hbar\beta; x_a, 0)$ contains only the connected Feynman diagrams. We obtain from (6) and (23)–(25) the expansion

$$\begin{aligned}
 W(x_b, \hbar\beta; x_a, 0) = & -\frac{g}{\hbar} \left(\begin{array}{c} \times \\ | \\ \times \end{array} + 6 \begin{array}{c} \circ \\ | \\ \times \end{array} + 3 \begin{array}{c} \circ \\ \circ \end{array} \right) \\
 & + \frac{g^2}{2\hbar^2} \left(8 \begin{array}{c} \times \\ | \\ \times \end{array} \begin{array}{c} \times \\ | \\ \times \end{array} + 36 \begin{array}{c} \times \\ \diagdown \\ \times \end{array} \begin{array}{c} \circ \\ \circ \end{array} + 48 \begin{array}{c} \times \\ | \\ \times \end{array} \begin{array}{c} \circ \\ | \\ \times \end{array} \right. \\
 & + 48 \begin{array}{c} \circ \\ | \\ \times \end{array} + 72 \begin{array}{c} \circ \\ | \\ \times \end{array} \begin{array}{c} \circ \\ | \\ \times \end{array} + 72 \begin{array}{c} \times \\ \diagdown \\ \times \end{array} \begin{array}{c} \circ \\ \circ \end{array} \\
 & \left. + 36 \begin{array}{c} \circ \\ \circ \\ \circ \end{array} + 12 \begin{array}{c} \circ \\ \circ \end{array} \right) + \dots, \quad (26)
 \end{aligned}$$

where disconnected diagrams are indeed no longer present. As mentioned above, we restrict ourselves to the low-temperature limit of the diagonal elements of the density matrix which determine the ground-state wave function. In order to evaluate the various contributions in (26), we need the classical path (12) and the Green function (13) in the low-temperature limit:

$$\begin{aligned}
 \lim_{\beta \rightarrow \infty} x_{cl}(\tau) & = x \left(e^{-\omega\tau} + e^{-\omega(\hbar\beta-\tau)} \right) , \quad (27) \\
 \lim_{\beta \rightarrow \infty} G(\tau_1, \tau_2) & = \frac{\hbar}{2M\omega} \left[\theta(\tau_1 - \tau_2) e^{-\omega(\tau_1-\tau_2)} + \theta(\tau_2 - \tau_1) e^{-\omega(\tau_2-\tau_1)} \right]
 \end{aligned}$$

$$\left. -e^{-\omega(\tau_1+\tau_2)} - e^{-2\hbar\beta\omega+\omega(\tau_1+\tau_2)} \right]. \quad (28)$$

Computing with these expressions the Feynman diagrams in (26), the low-temperature limit of the imaginary-time evolution amplitude (25) reads together with (11)

$$\begin{aligned} \lim_{\beta \rightarrow \infty} \langle x | \hbar\beta | x \rangle &= \lim_{\beta \rightarrow \infty} \sqrt{\frac{M\omega}{\hbar\pi}} \exp \left[-\frac{\hbar\beta\omega}{2} - \frac{M\omega}{\hbar} x^2 + \frac{g}{\hbar} \left(\frac{9\hbar^2}{8M^2\omega^3} \right. \right. \\ &\quad \left. \left. - \frac{3\hbar^3\beta}{4M^2\omega^2} - \frac{3\hbar}{2M\omega^2} x^2 - \frac{1}{2\omega} x^4 \right) + \frac{g^2}{2\hbar^2} \left(\frac{21\hbar^5\beta}{4M^4\omega^5} - \frac{205\hbar^4}{16M^4\omega^6} \right. \right. \\ &\quad \left. \left. + \frac{21\hbar^3}{2M^3\omega^5} x^2 + \frac{11\hbar^2}{4M^2\omega^4} x^4 + \frac{\hbar}{3M\omega^3} x^6 \right) + \dots \right]. \quad (29) \end{aligned}$$

According to (5), the partition function Z follows from (29) by performing an integration with respect to x . This results in

$$\lim_{\beta \rightarrow \infty} Z = \lim_{\beta \rightarrow \infty} \exp \left(-\frac{\hbar\beta\omega}{2} - \frac{3g\hbar^2\beta}{4M^2\omega^2} + \frac{21g^2\hbar^3\beta}{8M^4\omega^5} + \dots \right). \quad (30)$$

Inserting (29) and (30) into (3) we observe a cancellation of all terms which would diverge in the low-temperature limit $\beta \rightarrow \infty$. Thus the diagonal elements of the density matrix read in this limit

$$\begin{aligned} \lim_{\beta \rightarrow \infty} \rho(x, x) &= \sqrt{\frac{M\omega}{\hbar\pi}} \exp \left[-\frac{M\omega}{\hbar} x^2 + \frac{g}{\hbar} \left(\frac{9\hbar^2}{8M^2\omega^3} - \frac{3\hbar}{2M\omega^2} x^2 - \frac{1}{2\omega} x^4 \right) \right. \\ &\quad \left. + \frac{g^2}{2\hbar^2} \left(-\frac{205\hbar^4}{16M^4\omega^6} + \frac{21\hbar^4}{2M^3\omega^5} x^2 + \frac{11\hbar^2}{4M^2\omega^4} x^4 + \frac{\hbar}{3M\omega^3} x^6 \right) + \dots \right]. \quad (31) \end{aligned}$$

By taking the square root and expanding the exponential term up to second order in the coupling strength g , we derive the second-order ground-state wave function (2):

$$\begin{aligned} \Psi(x) &= \left(\frac{M\omega}{\hbar\pi} \right)^{1/4} \exp \left(-\frac{M\omega}{2\hbar} x^2 \right) \left[1 - \frac{g}{\hbar} \left(-\frac{9\hbar^2}{16M^2\omega^3} \right. \right. \\ &\quad \left. \left. + \frac{3\hbar}{4M\omega^2} x^2 + \frac{1}{4\omega} x^4 \right) + \frac{g^2}{2\hbar^2} \left(-\frac{1559\hbar^4}{256M^4\omega^6} + \frac{141\hbar^3}{32M^3\omega^5} x^2 \right. \right. \\ &\quad \left. \left. + \frac{53\hbar^2}{32M^2\omega^4} x^4 + \frac{13\hbar}{24M\omega^3} x^6 + \frac{1}{16\omega^2} x^8 \right) + \dots \right]. \quad (32) \end{aligned}$$

This result corresponds to the solution of the Bender-Wu recursion relation [7] for the ground-state wave function which is normalized such that

$$\int_{-\infty}^{+\infty} dx \Psi^2(x) = 1 \quad (33)$$

holds up to second order in the coupling strength g .

3 Variational Perturbation Theory

Variational perturbation theory enables us to evaluate the ground-state wave function for all values of the coupling constant g and even in the strong-coupling limit $g \rightarrow \infty$. To this end we simply add and subtract a harmonic oscillator of trial frequency Ω to the anharmonic oscillator potential (1):

$$V(x) = \frac{M}{2}\Omega^2x^2 + g\frac{M}{2}\frac{\omega^2 - \Omega^2}{g}x^2 + gx^4. \quad (34)$$

We now treat the second term as if it was of the order of the coupling constant g . The result is obtained most simply by substituting the frequency ω in the original anharmonic oscillator potential (1) according to Kleinert's square root trick [1]

$$\omega \rightarrow \Omega\sqrt{1+gr}, \quad (35)$$

where we have

$$r \equiv \frac{\omega^2 - \Omega^2}{g\Omega^2}. \quad (36)$$

Writing the ground-state wave function (32) in the form $\Psi(x) = \exp[W(x)]$ with the cumulant expansion

$$W(x) = \exp \left[\frac{1}{4} \log \left(\frac{M\omega}{\hbar\pi} \right) - \frac{M\omega}{2\hbar}x^2 + \frac{g}{\hbar} \left(\frac{9\hbar^2}{16M^2\omega^3} - \frac{3\hbar}{4M\omega^2}x^2 - \frac{1}{16\omega}x^4 \right) + \frac{g^2}{2\hbar^2} \left(-\frac{205\hbar^4}{32M^4\omega^6} + \frac{21\hbar^4}{4M^3\omega^5}x^2 + \frac{11\hbar^2}{8M^2\omega^4}x^4 + \frac{\hbar}{6M\omega^3}x^6 \right) + \dots \right], \quad (37)$$

we apply the trick (35) to $W(x)$, and reexpand in powers of g at fixed r . Afterwards r is substituted according to (36). Thus we obtain in the first order

$$\Psi^{(1)}(x, \Omega) = \exp \left[\frac{1}{4} \log \left(\frac{M\Omega}{\hbar\pi} \right) - \frac{1}{8} + \frac{\omega^2}{8\Omega^2} - \frac{M\Omega}{4\hbar} \left(1 + \frac{\omega^2}{\Omega^2} \right) x^2 \right]$$

$$+\frac{g}{\hbar} \left(\frac{9\hbar^2}{16M^2\Omega^3} - \frac{3\hbar}{4M\Omega^2}x^2 - \frac{1}{4\Omega}x^4 \right) \Big], \quad (38)$$

whereas the second-order expansion reads

$$\begin{aligned} \Psi^{(2)}(x, \Omega) = \exp \Big\{ & \frac{1}{4} \log \left(\frac{M\Omega}{\hbar\pi} \right) - \frac{1}{16} + \frac{\omega^2}{4\Omega^2} - \frac{\omega^4}{16\Omega^4} \\ & - \frac{M\Omega}{2\hbar} \left(\frac{3}{8} + \frac{3\omega^2}{4\Omega^2} - \frac{\omega^4}{8\Omega^4} \right) x^2 + \frac{g}{\hbar} \left[\frac{9\hbar^2}{16M^2\Omega^3} \left(\frac{5}{2} - \frac{3\omega^2}{2\Omega^2} \right) \right. \\ & \left. - \frac{3\hbar}{4M\Omega^2} \left(2 - \frac{\omega^2}{\Omega^2} \right) x^2 - \frac{1}{4\Omega} \left(\frac{3}{2} - \frac{\omega^2}{2\Omega^2} \right) x^4 \right] \\ & \left. + \frac{g^2}{2\hbar^2} \left[-\frac{205\hbar^4}{32M^4\Omega^6} + \frac{21\hbar^3}{2M^3\Omega^5}x^2 + \frac{11\hbar^2}{8M^2\Omega^4}x^4 + \frac{\hbar}{6M\Omega^3}x^6 \right] \right\}. \quad (39) \end{aligned}$$

Both in first and in second order, the ground-state wave function depends on the artificially introduced frequency parameter Ω . According to the principle of minimal sensitivity [8] we minimize its influence on $\Psi^{(n)}(x, \Omega)$ by searching for local extrema of $\Psi^{(n)}(x, \Omega)$ with respect to Ω . As we have written the wave function in the form $\Psi^{(n)}(x, \Omega) = \exp[W^{(n)}(x, \Omega)]$, it is sufficient to take into account just the inner derivative of $\Psi^{(n)}(x, \Omega)$, i.e. we obtain the condition $\partial W^{(n)}(x, \Omega)/\partial\Omega = 0$.

It turns out in the first order $n = 1$ that this equation has two solutions for $x < 0.684$ and for $x > 0.780$, however in the interval $0.684 < x < 0.780$, $\Psi^{(1)}(x, \Omega)$ does not have any extremum [4]. In accordance with the principle of minimal sensitivity we look for turning points on that interval instead, i.e. we solve $\partial^2 W^{(1)}(x, \Omega)/\partial\Omega^2 = 0$. Fig. 1 shows how the curve for the turning points links the extremal branches. Now we have to choose which one of the branches of $\Omega^1(x)$ we take into account. Inserting the lower branch for $x > 0.780$ into the wave function (38) leads to unphysical results as the ground-state wave function explodes dramatically. Thus we choose the upper branch for $x > 0.780$. For $x < 0.684$ the wave function becomes rather independent of the choice of Ω . As we are looking for a function $\Omega^{(1)}(x)$ which is as smooth as possible, we choose the lower branch for $x < 0.684$. Fig. 1 shows all branches of Ω and highlights our final choice by a solid line.

For the second order $n = 2$ there are no real positive solutions of the equation $\partial W^{(2)}(x, \Omega)/\partial\Omega = 0$ on the interval $x = [0, 4]$. Once more we have to look for turning points instead and solve $\partial^2 W^{(2)}(x, \Omega)/\partial\Omega^2 = 0$. This equation has two positive solutions on this interval, so we get two branches for the solution $\Omega^{(2)}(x)$ (see Fig. 2). Again we have to choose one of these two

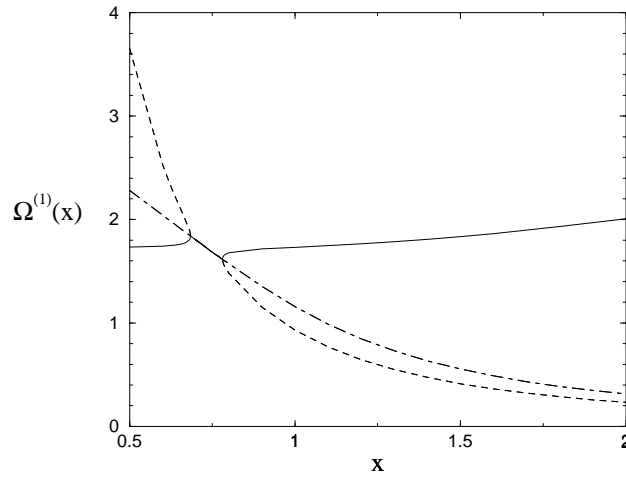


Figure 1. First-order results for the variational parameter Ω at the intermediate coupling $g = 1/2$. The extremal branches for $x < 0.684$ and for $x > 0.780$ (solid lines and dashed lines) are obtained from the equation $\partial W^{(1)}(x, \Omega)/\partial \Omega = 0$. For $0.684 < x < 0.780$ there are no real positive solutions of this equation. Thus we look in this interval also for turning points, i.e. we determine real positive solutions of the equation $\partial^2 W^{(1)}(x, \Omega)/\partial \Omega^2 = 0$. The curve for the turning points on the entire interval lies between the two other branches (dot-dashed line) and fills the gap. Thus we can take those branches into account which provide us with the most continuous function $\Omega^{(1)}(x)$, i.e. the solid line.

branches. Relying on a similar argument as for the first-order approximation we choose the upper branch for $x > 0.8$ and the lower one for $x < 0.8$. The perturbation series converges so quickly that the curves for the first and second order as well as the exact ground-state wave function are not distinguishable on the plots. To see the difference we determine the mean square deviation from the exact numerical solution

$$D^{(n)} = 2 \int_0^\infty dx \left[\Psi^{(n)}(x) - \Psi^{\text{ex}}(x) \right]^2, \quad (41)$$

where the index n denotes the order. The integration is performed numerically. The factor 2 is introduced for symmetry reasons, since we restrict our calculations to the positive x -axis. It turns out that the mean square deviation $D^{(2)} = 6.8 \times 10^{-7}$ is smaller than $D^{(1)} = 1.1 \times 10^{-5}$ by a factor of 0.063, which indicates that variational perturbation theory converges very quickly also for the ground-state wave function. The same applies to both

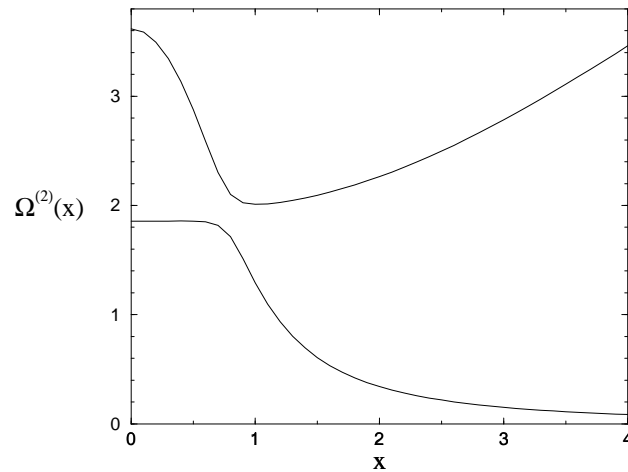


Figure 2. The two positive branches of $\Omega^{(2)}(x)$ on the interval $[0, 4]$ for intermediate coupling $g = 1/2$ obtained by solving the turning point equation $\partial^2 W^{(2)}(x, \Omega) / \partial \Omega^2 = 0$. In order to achieve the smoothest function we choose the lower branch for $x < 0.8$ and the upper branch for $x > 0.8$. This choice is justified by the results of our first-order calculation (see Fig. 1).

weak and strong coupling as is illustrated in Fig. 3 which shows the second-order ground-state wave function $\Psi^{(2)}(x)$ for $g = 0.1$, $g = 1/2$, and $g = 50$, respectively.

Note that variational perturbation theory does not preserve the normalization of the wave function. Although the perturbative ground-state wave function (32) is still normalized in the usual sense, this normalization is spoiled by extremizing $\Psi(x, \Omega)$ with respect to the frequency parameter Ω . Thus we have to normalize the variational ground-state wave function at the end.

Acknowledgments

Both of us congratulate Professor Kleinert to his 60th birthday. F.W. thanks Professor Kleinert for supervising the research for his diploma thesis where the results of this article were derived. Moreover F.W. is very grateful to his family for their patience and their support. Finally both authors thank Michael Bachmann who always found time for fruitful discussions on variational perturbation theory.

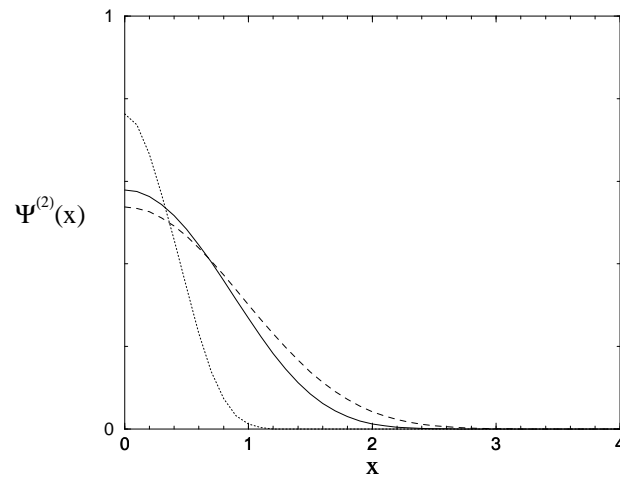


Figure 3. The normalized second-order ground-state wave function for weak coupling (dashed, $g = 0.1$), for intermediate coupling (solid, $g = 1/2$), and for strong coupling (dotted, $g = 50$).

References

- [1] H. Kleinert, *Path Integrals in Mechanics, Statistics, and Polymer Physics*, 2nd ed. (World Scientific, Singapore, 1995).
- [2] W. Janke and H. Kleinert, *Phys. Rev. Lett.* **75**, 2787 (1995).
- [3] H. Kleinert and W. Janke, *Phys. Lett. A* **206**, 283 (1995).
- [4] T. Kunihiro, *Phys. Rev. Lett.* **78**, 3229 (1997).
- [5] M. Bachmann, H. Kleinert, and A. Pelster, *Phys. Rev. A* **60**, 3429 (1999).
- [6] H. Kleinert, A. Pelster, and M. Bachmann, *Phys. Rev. E* **60**, 2510 (1999).
- [7] C.M. Bender and T.T. Wu, *Phys. Rev.* **184**, 1231 (1969); *Phys. Rev. D* **7**, 1620 (1973).
- [8] P.M. Stevenson, *Phys. Rev. D* **23**, 2916 (1981).